

# Topological swing in Bloch oscillations

Lavi K. Upreti,<sup>1</sup> C. Evain,<sup>2</sup> S. Randoux,<sup>2</sup> P. Suret,<sup>2</sup> A. Amo,<sup>2</sup> and P. Delplace<sup>1</sup>

<sup>1</sup>*Univ Lyon, ENS de Lyon, Univ Claude Bernard, CNRS, Laboratoire de Physique, F-69342 Lyon, France*

<sup>2</sup>*Univ. Lille, CNRS, UMR 8523 – PhLAM – Physique des Lasers Atomes et Molécules, F-59000 Lille, France*

(Dated: March 26, 2025)

Bloch oscillations are a fundamental property of wavepackets subject to an external field in a lattice. The period of oscillation is set by the magnitude of this field, and it is independent of the shape and the nature of the band in which the wavepacket is created. Here we show that Bloch oscillations can be directly related to a topological invariant. This invariant characterizes the evolution operators describing the wavepacket evolution under a gauge transformation. Using a general Floquet framework to describe quantum walks, we unveil a new class of sub-oscillations within a Bloch period, whose number is given by the topological invariant. Our findings allow a direct implementation in photonic setups, which provide a new protocol to measure certain topological invariants.

Bloch oscillations, the oscillatory motion of an electron subject to a constant electric field in a periodic potential, are one of the most fascinating effects of adiabatic quantum transport. Initially introduced by Zener in the context of quantum electrons in crystals [1, 2], Bloch oscillations are found in a wide variety of physical systems such as semiconductor superlattices [3–5], trapped cold atoms [6] and photonics systems [7, 8]. From fractional Bloch oscillations [9, 10] to super Bloch oscillations [11, 12], their declension reveals the richness of wavepackets dynamics in periodic structures, captured within a simple semiclassical picture. A recent case of interest has been the study of Bloch oscillations in bands with nontrivial Berry curvature [13–18] or Berry-Zak phases [19]. In this case, the geometrical or topological properties of the bands alter the oscillation dynamics and can give rise to intricate wavepacket evolutions.

The appearance of anomalous velocities and other topological effects in a lattice subject to periodic driving is another striking property of wavepacket dynamics. From quantized Thouless pumping to Floquet topological insulators, periodically driving a parameter in lattice Hamiltonians has proved to be a very powerful way of generating nontrivial topological features. A fundamental question is whether Bloch oscillations can appear in Hamiltonians subject to periodic driving and whether such oscillations can possess topological traits. Bloch oscillations have indeed been considered in the context of cyclic driving in photonic [8, 20] but their eventual relation to topological invariants remains to be established.

In a lattice Hamiltonian subject to a periodic drive, different regimes can be encountered depending on the frequency-scale of the driving in comparison to the hopping energy between sites. At high frequencies, a clever driving of the Hamiltonian gives rise to an artificial gauge field and the appearance of bands characterized by a non-zero Chern number [21, 22]. At frequencies comparable to the hopping energies, the cyclic driving can give rise to anomalous topological phases, characterized by topological gap invariants with unidirectional [23] or helical

[24] edge states. At further lower frequencies, in the adiabatic regime, phenomena such as Thouless pumping results in the quantized drift of particles [25, 26]. The drift originates from the anomalous group velocity intimately related to the Berry curvature of the Bloch bands, and can be used to measure it [27–32]. Remarkably, the manifestation of the Berry curvature through the motion of wavepackets is one of the few existing tools to probe the geometrical and topological properties of the bulk bands [33], even in non-periodic systems [34, 35]. These examples show the intimate relationship between periodic driving and the emergence of geometrical and topological properties of wavepackets in a lattice.

Here we establish a connection between Bloch oscillations and the topological features associated with periodic driving. We report a new topological property of the motion of a wavepacket in a lattice subject to a cyclic driving that manifests in a new class of Bloch *sub*-oscillations. We use a general Floquet framework to describe 1D quantum walks that is accessible in current photonic setups. Remarkably, both the usual Bloch oscillations and the sub-oscillations are found to be governed by a winding number of the evolution operator and are, therefore, of topological origin. Our framework provides a clear picture of the interplay between this topological *swing* and standard Bloch oscillations. It establishes a strong parallel between Bloch oscillations and Thouless pumping as they both reflect two complementary topological aspects of wavepackets dynamics.

The model we consider is sketched in Fig. 1. It consists of an oriented scattering network that describes a periodic discrete-time evolution of a quantum state or a wavepacket. The links between the nodes of the network have a preferential orientation (from top to bottom) that accounts for the direction of the flow with the time of an input signal. It is thus formally equivalent to a 1D quantum walk and describes, for instance, the evolution of a light pulse injected in a 1D lattice of birefringent beamsplitters [36], periodically coupled waveguides [37] or coupled fiber rings [32, 38]. At each time step  $j$  and

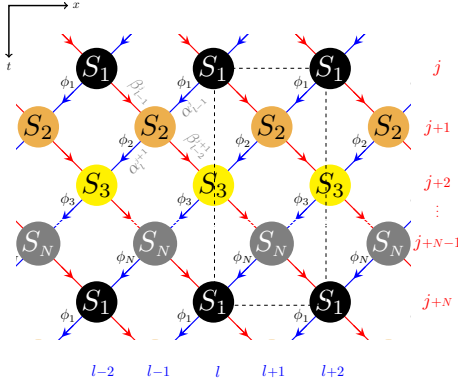


Figure 1. 2D oriented scattering lattice where the vertical axis plays the role of time. A dashed rectangle emphasizes the unit cell of this lattice.

position  $l$ , the scattering of the wave amplitudes along the rightward  $\alpha_l^j$  and leftward  $\beta_l^j$  links occurs at a node of coordinates  $(l, j)$ , and is parametrized by a dimensionless parameter  $\theta_j$  entering the unitary matrix

$$S_j = \begin{pmatrix} \cos \theta_j & i \sin \theta_j \\ i \sin \theta_j & \cos \theta_j \end{pmatrix}. \quad (1)$$

In addition to these scattering processes, we introduce a phase shift  $\phi_j$  carried along by the states in each link, as in [32]. Without any loss of generality, we consider a non-zero phase shift for the leftward states only (in blue in Fig. 1). The key point is that the value of this phase is allowed to vary at each time step  $j$  within a cyclic time period of  $N$  steps. It can, therefore, be regarded as a periodic driving parameter of the scattering matrix. The outgoing amplitudes at time  $j+1$  are related to the incoming amplitudes at time  $j$  as

$$\begin{aligned} \alpha_l^{j+1} &= (\cos \theta_j \alpha_{l+1}^j + i \sin \theta_j \beta_{l+1}^j) e^{i\phi_j} \\ \beta_l^{j+1} &= (i \sin \theta_j \alpha_{l-1}^j + \cos \theta_j \beta_{l-1}^j). \end{aligned} \quad (2)$$

Assuming discrete translation invariance along the  $x$ -direction, the system can be treated in the Bloch-Floquet formalism. The corresponding (Floquet) unitary evolution operator after a periodic sequence of  $N$  steps reads:

$$U_F(k, \{\phi_j\}) = (B_{\text{mod}(N,2)} S_N D_N) \dots (B_0 S_2 D_2) (B_1 S_1 D_1), \quad (3)$$

$$B_1 = \begin{pmatrix} 1 & 0 \\ 0 & e^{-ik} \end{pmatrix}, \quad B_0 = \begin{pmatrix} e^{ik} & 0 \\ 0 & 1 \end{pmatrix}, \quad D_j = \begin{pmatrix} e^{i\phi_j} & 0 \\ 0 & 1 \end{pmatrix}$$

where  $k$  is the (dimensionless) quasimomentum in the  $x$ -direction. The eigenvalues of Eq. 3 decompose as  $\lambda = e^{i\varepsilon}$ , where  $\varepsilon$  will be hereafter referred to as the (dimensionless) quasienergy. The phases  $\phi_j$  are chosen to be proportional to a phase of reference  $\phi$  by a rational number, i.e.  $\phi_j = (m_j/n_j)\phi$ . The Floquet operator  $U_F(k, \phi)$  then depends on two periodic variables, the quasimomentum

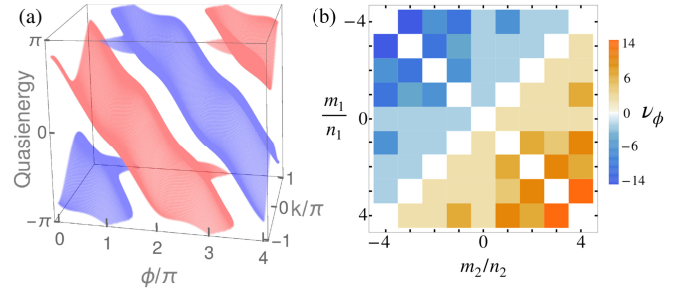


Figure 2. (a) Quasienergy spectrum with a winding  $\nu_\phi = -2$  obtained for a scattering model with two-steps per period for  $\theta_1 = \pi/4$ ,  $\theta_2 = \pi/4 - 0.6$ ,  $\phi_1 = \phi$  and  $\phi_2 = -2\phi$ . (b) Values of  $\nu_\phi$  for integer values of  $m_i/n_i$ .

$k$  and the phase  $\phi$ , which can be considered as a synthetic dimension. Thus, the quasienergies  $\varepsilon(k, \phi)$  span a synthetic 2D Brillouin zone (BZ). Note that for two-steps period ( $S_1$  and  $S_2$  in Fig. 1,  $N = 2$ ), the system reduces to former models studied experimentally in topological photonics, such as arrays of coupled waveguides with  $\phi = 0$ , where topological anomalous edge states were observed [37], and coupled fiber loops with  $\phi_2 = -\phi_1$  (zero net phase over a period), where the Berry curvature of the synthetic bands was measured [32].

An interesting situation arises when imposing a pattern of phase shifts  $\phi_j$  along a time period of  $N$  steps such that the net phase  $\phi_{\text{net}} \equiv \sum_{j=1}^N \phi_j$  does not vanish. This is the phase gained after a period, and it can be interpreted as a periodic kick when considering the dynamics of a wavepacket. The condition  $\phi_{\text{net}} \neq 0$  breaks inversion symmetry in the synthetic dimension  $\phi$ . Hence, in the full synthetic BZ, it also breaks the generalized inversion symmetry  $U_F(-k, -\phi) = \sigma_x U_F(k, \phi) \sigma_x$ , with  $\sigma_x$  being the standard Pauli matrix (see Ref. [39]). Remarkably, this symmetry breaking leads to a winding of all the quasienergy bands with respect to  $\phi$ , as illustrated in Fig. 2(a). A similar quasienergy winding was reported when considering periodically driven trapped cold atoms with a different protocol [40].

For simplicity, let us keep our focus on two-steps period ( $N = 2$ ), so that the two distinct phase shifts at each step read  $\phi_1 = (m_1/n_1)\phi$  and  $\phi_2 = (m_2/n_2)\phi$ . The size of the BZ in the  $\phi$  dimension thus depends on the choice of  $m_i$  and  $n_i$ . Let us introduce the period  $\Phi$  of the quasienergy with respect to the phase variable i.e.  $\varepsilon(k, \phi + \Phi) = \varepsilon(k, \phi)$ . This period is related to the least common multiple (LCM) of a combination of  $m_i$  and  $n_i$  in the following way  $\Phi = 4\pi \text{LCM}[(m_1/n_1 - m_2/n_2)^{-1}, (m_1/n_1 + m_2/n_2)^{-1}]$  (see Ref. [39]). This allows us to define the winding of the quasienergies along  $\phi$  as

$$\nu_\phi \equiv \sum_{p=1}^N \frac{1}{2\pi} \int_0^\Phi d\phi \frac{\partial \varepsilon_p(k, \phi)}{\partial \phi}. \quad (4)$$

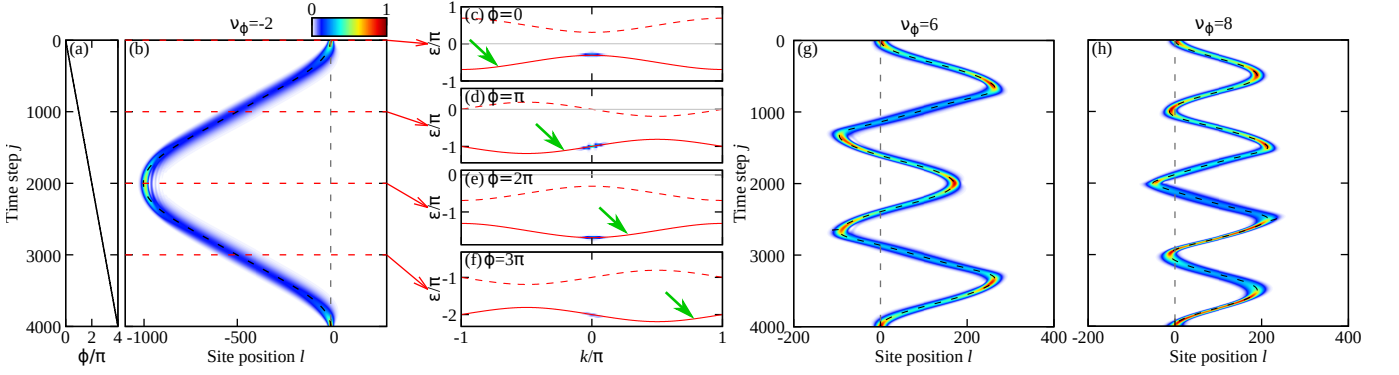


Figure 3. (a) Adiabatic increase of  $\phi$  leads to (b) a standard Bloch oscillation ( $\nu_\phi = -2$ ), and to (g),(h) Bloch oscillation with sub-oscillations ( $\nu_\phi = 6$  and  $\nu_\phi = 8$  respectively) of a wavepacket injected in the scattering network at time  $j = 0$  and position  $l = 0$ . Color scale: intensity ( $|\alpha_l^j|^2 + |\beta_l^j|^2$ ) of the wavepacket, injected with a Gaussian shape (with a rms width of 10 sites) in one band [the blue band shown in Fig. 2(a) for the case of (b)]. Dashed black line: analytical calculation of the centre of mass motion of a wavepacket from Eq. (32) in Ref. [39]. (b),(g),(h) show one period  $T_B$  of oscillation for the values of  $(m_1, m_2, n_1, n_2), \theta_1, \theta_2$  as  $(1, -2, 1, 1), \pi/4, \pi/4 - 0.5$  for (b);  $(4, -1, 1, 1), \pi/4, \pi/4 - 0.2$  for (g); and  $(9, -1, 2, 2), \pi/4, \pi/4 - 0.2$  for (h). In (c)-(f), the norm of the 2D Fourier transform of the wavepacket ( $\alpha$  part) after having evolved to the time step indicated by the horizontal lines in (b), and both the solid and the dashed red lines represent numerically calculated bands [Eq. (24) in Ref. [39]]. The vertical scales differ in each panel, where the green arrows show the direction in which the bands wind when  $\phi$  increases.

This winding number is a topological property of the Floquet evolution operator, as it reads as an element of the homotopy group  $\pi_1[U(N)] = \mathbb{Z}$

$$\nu_\phi = \frac{1}{2\pi i} \int_0^\Phi d\phi \operatorname{tr} \left[ U_F^{-1} \partial_\phi U_F \right] \in 2\mathbb{Z}. \quad (5)$$

Note that this is an even integer in our specific case due to the even number of bands (two) in our model. A direct calculation leads to the simple result

$$\nu_\phi = \frac{\Phi}{2\pi} \left( \frac{m_1}{n_1} + \frac{m_2}{n_2} \right), \quad (6)$$

which remarkably does not depend either on  $k$  (since the winding of a quasienergy band  $\varepsilon_p(k, \phi)$  along  $\phi$  must be the same for any  $k$ ) or on the scattering amplitudes  $\theta_j$ . Instead, it is proportional to the net phase  $(\phi_1 + \phi_2)/\phi$  that breaks inversion symmetry. A phase diagram representing the different possible values of  $\nu_\phi$  as a function of  $m_i/n_i$  is shown in Fig. 2(b).

A striking consequence of the winding of the quasienergy bands is the unconventional dynamics of the wavepackets in position space when adiabatically increasing the coordinate  $\phi$ . In the following, we show how these dynamics reveal a new kind of Bloch oscillations described by the winding number  $\nu_\phi$ . Figure 3(b) shows the  $j$ -time evolution of a Gaussian wavepacket injected at  $j = 0$  in the blue band of Fig. 2(a) at  $k = 0$ , when  $\phi$  is adiabatically increased from 0 to  $\Phi = 4\pi$ , with  $\phi(j) = \gamma_0 j$  where the rate  $\gamma_0 = 2\pi/2000$  [see Fig. 3(a)]. To compute the spatio-temporal dynamics, we apply Eq. (2) to the initial wavepacket. The wavepacket periodically oscillates in space coordinate while keeping  $k$  constant.

This can be readily seen in Fig. 3(c)-(f), where we show the 2D Fourier transform of the wavepacket after having evolved to the time step indicated by the horizontal lines in Fig. 3(b). These panels provide a phenomenological understanding of the mechanism behind the oscillations: as  $\phi$  is adiabatically increased, the band dispersions are displaced in a diagonal direction in  $(k, \varepsilon)$  space [green arrows in Fig. 3(c)-(f)], a direct consequence of the winding of the bands (see also figure 2(a)). Therefore, the group velocity  $v_g = \frac{\partial \varepsilon}{\partial k}$  of a wavepacket with a given  $k$  changes sign when  $\phi(j)$  increases, resulting in oscillations in the spatial coordinate.

It is worth stressing that two distinct drivings are present in our model: (i) a fast cyclic driving of the phases  $\phi_1, \phi_2$  within a Floquet period, which confers a nontrivial winding to the bands; (ii) a slow adiabatic increase of the phase  $\phi$  which results in the oscillations. An analytical calculation of the centre of mass trajectory  $X_c(t, k)$  of the wavepacket initially injected at a given  $k$  can be inferred from the group velocity of the quasienergy bands in parameter space (see Ref. 39):

$$X_c(t, k) = \gamma_0 \int_0^t d\tau v_g(\phi(\tau), k), \quad (7)$$

where the continuous-time variable  $t$  extrapolates the discrete one  $j$ . This semiclassical trajectory is shown in black dashed lines in Fig. 3(b), which fits the simulation plot perfectly.

More importantly, the observed oscillatory phenomenon establishes a direct connection between the winding of the bands in our Floquet-Bloch model and the usual Bloch oscillations in a periodic crystal subject to a constant electric field. Indeed, the adiabatic increase

of the phase shift  $\phi$  at a rate  $\gamma_0$  when the time steps  $j$  increases is analogous to a time-dependent vector potential that induces a (fictitious) electric field [41]  $E$  and, therefore, should result in Bloch oscillations. This was already noticed in the case of a single-step time evolution ( $N = 1$ ) by Wimmer and co-workers [8], who reported a gauge transformation relating the dynamics of a wavepacket in a lattice subject to a static potential gradient (i.e., a constant electric field), and the dynamics in a lattice subject to an adiabatic increase of the parameter  $\phi$  (see also [39]). To establish the connection between the winding of the quasienergy bands and Bloch oscillations, we note that, according to Eq. (7), the time periodicity  $T_B$  of the center of mass motion  $X_c$  is inherited from the periodicity of the quasienergy with respect to  $\phi$ . Accounting for the rate  $\gamma_0$  between time and phase variables, one infers that  $T_B = \Phi/\gamma_0$ . This directly relates the time period of the oscillations to the winding number associated to the quasienergy bands via Eq. (6) as

$$T_B = \frac{2\pi}{\gamma_0} \frac{\nu_\phi}{\frac{m_1}{n_1} + \frac{m_2}{n_2}}, \quad (8)$$

where negative values of  $\nu_\phi$  correspond to mirror symmetric trajectories to those with  $|\nu_\phi|$ .

In Eq. (8), we recognize the usual period  $T_B$  for Bloch oscillations induced by an average constant electric field  $E = (E_1 + E_2)/2$  where  $E_j = \frac{m_j \gamma_0}{n_j}$  is the fictitious electric field applied during the time step  $j$  (see Ref. [39] for more details), except that in Eq. (8), this standard relation is modified by the winding number  $\nu_\phi$ . In particular, the period  $T_B = 2\pi/E$  of the usual Bloch oscillations is recovered for  $|\nu_\phi| = 2$ , a situation in which each band winds once, as reported in Figs. 2(a) and 3(b).

Beyond this standard case, our model predicts a novel kind of topological oscillations: higher winding numbers may not only change the period  $T_B$ , but also yield more complex oscillations with additional turning points within  $T_B$ . Two examples are shown in Fig. 3(g-h) for values of  $m_i, n_i$  resulting in bands of windings  $\nu_\phi = 6$  and 8, respectively, and same oscillating period  $T_B$  as in Fig. 3(b). Remarkably, in a period  $T_B$ , the number of turning points is found to be precisely  $\mathcal{N}_t = |\nu_\phi|$  (see Ref. [39]). This result confers a topological nature to Bloch oscillations. Note that the standard ones simply have two turning points per period (see Fig. 3(b)), in agreement with  $\mathcal{N}_t = 2 = |\nu_\phi|$ .

So far, we have considered windings of the bands induced by periodic pumping in the synthetic dimension. We now show that a winding of the quasienergy bands along the  $k$ -direction can similarly be induced when inversion symmetry is broken in the spatial dimension, and it results in a different topological phenomenon: quantized displacement of the mean particle position. This effect can be straightforwardly implemented in scattering network models by connecting next-nearest neighbor

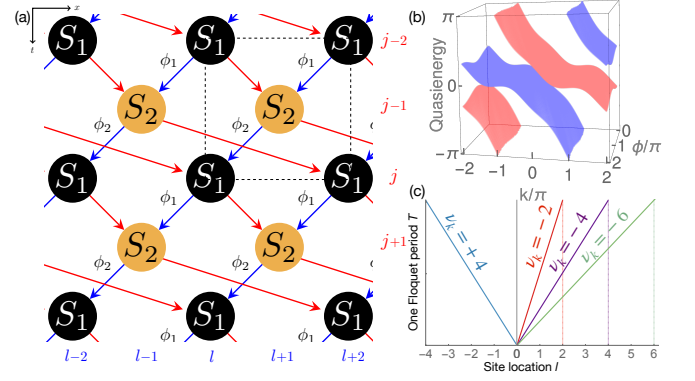


Figure 4. (a) Two-steps scattering network with the next nearest coupling in the second step. A dashed black rectangle emphasizes the unit cell of this lattice. (b) Quasienergy bulk spectrum for the model depicted in (a) with  $\theta_1 = \pi/4$ ,  $\theta_2 = \pi/4 - 0.6$  and  $\phi_1 = -\phi_2$ . (c) Quantized displacement of the mean particle position with associated winding numbers  $\nu_k$ .

nodes, as sketched in Fig. 4(a) for a two-step time evolution (see Ref. [39] for the step evolution equations). For the sake of generality, we have kept the phase  $\phi_j$ , which we take as  $\phi_1 = \phi = -\phi_2$ , such that  $\nu_\phi = 0$ , i.e., there are no Bloch oscillations. The corresponding quasienergy bands, displayed in Fig. 4(b), show a winding along  $k$  for each  $\phi$ . This feature is captured by a winding number of the Floquet operator along  $k$ , analogous to that defined in Eqs. (4)-(5) for  $\phi$ . More generally, when considering even further long range couplings, this winding number is found to read [39]:

$$\nu_k = \frac{\kappa}{2\pi} \left( \frac{r_1}{s_1} + \frac{r_2}{s_2} \right) \quad (9)$$

where  $\kappa$  is the periodicity of the bands in  $k$  and  $r_j/s_j$  is related to the range of the couplings between nodes to the left or to the right at each time step  $j$ . For the case illustrated in Fig. 4(a),  $r_1/s_1 = 1$ ,  $r_2/s_2 = -2$ .

In the spirit of the seminal work of Thouless [25], and as revisited by Kitagawa *et al.* [26] within the Floquet formalism, this winding number  $\nu_k$  can be related to the mean displacement of particles after  $P$  Floquet periods  $T$ , in a state where all the bands are uniformly excited, that is [39]:

$$\Delta x = -P \frac{2\pi}{\kappa} \nu_k \quad (10)$$

Despite this apparent similarity, this quantized transport property differs from the usual Thouless pumping that results from an *adiabatic* driving of the system. In that case, the quantization can be expressed as a Chern number of the slowly driven instantaneous filled states parametrized over the effective 2D BZ  $(k, t)$ . This Chern number was later reinterpreted as a sum of the winding numbers in  $k$  over the filled bands [26]. In the adiabatic regime, if this sum runs over all the bands, as in our case,



then the Chern numbers of each band sum up to zero, and there is no drift. Quantized drifts obtained for our *non-adiabatic* scattering model are shown in Fig. 4(c). More generally, quasienergy windings along both  $\phi$  and  $k$  coordinates can coexist, leading to quite complex drifted Bloch oscillations for wavepackets shown in the Supplementary Material [39].

Our study unveils the topological aspects of Bloch oscillations and extends them to a family of oscillatory phenomena accessible in artificial systems such as arrays of photonic waveguides and coupled fibers. It generalizes straightforwardly to periodically driven lattices of ultracold atoms where a protocol to generate quasienergy windings and oscillations was proposed [40], although neither the winding number  $\nu_\phi$  nor its relation to the number of Bloch sub-oscillations was identified. This direct relation between the number of turning points within an oscillation period and the winding number of the bands provides a new protocol to measure topological invariants in systems described by a quantum walk.

*Acknowledgements*— The authors are thankful to Benoit Douçot for his very constructive comments. This work was supported by the French Agence Nationale de la Recherche (ANR) under grant Topo-Dyn (ANR-14-ACHN-0031), the Labex CEMPI (ANR-11-LABX-0007), the CPER Photonics for Society P4S, the I-Site ULNE project NONTOP and the *Métropole Européenne de Lille* via the project TFlight.

- 
- [1] F. Bloch, *Z. Phys.* **52**, 555 (1929).
  - [2] C. Zener and R. H. Fowler, *Proc. R. Soc. A* **145**, 523 (1934).
  - [3] P. Voisin, J. Bleuse, C. Bouche, S. Gaillard, C. Alibert, and A. Regreny, *Phys. Rev. Lett.* **61**, 1639 (1988).
  - [4] J. Feldmann, K. Leo, J. Shah, D. A. B. Miller, J. E. Cunningham, T. Meier, G. von Plessen, A. Schulze, P. Thomas, and S. Schmitt-Rink, *Phys. Rev. B* **46**, 7252 (1992).
  - [5] K. Leo, P. H. Bolivar, F. Brüggemann, R. Schwedler, and K. Köhler, *Solid State Commun.* **84**, 943 (1992).
  - [6] M. Ben Dahan, E. Peik, J. Reichel, Y. Castin, and C. Salomon, *Phys. Rev. Lett.* **76**, 4508 (1996).
  - [7] T. Pertsch, P. Dannberg, W. Elfle, A. Bräuer, and F. Lederer, *Phys. Rev. Lett.* **83**, 4752 (1999).
  - [8] M. Wimmer, M.-A. Miri, D. Christodoulides, and U. Peschel, *Sci. Rep.* **5**, 17760 (2015).
  - [9] F. Claro, J. F. Weisz, and S. Curilef, *Phys. Rev. B* **67**, 193101 (2003).
  - [10] G. Corrielli, A. Crespi, G. Della Valle, S. Longhi, and R. Osellame, *Nat. Comm.* **4**, 1555 (2013).
  - [11] A. Alberti, V. V. Ivanov, G. M. Tino, and G. Ferrari, *Nat. Phys.* **5**, 547 (2009).
  - [12] E. Haller, R. Hart, M. J. Mark, J. G. Danzl, L. Reichsöllner, and H.-C. Nägerl, *Phys. Rev. Lett.* **104**, 200403 (2010).
  - [13] S. Longhi, *Opt. Lett.* **32**, 2647 (2007).
  - [14] A. Szameit, F. Dreisow, M. Heinrich, R. Keil, S. Nolte, A. Tünnermann, and S. Longhi, *Phys. Rev. Lett.* **104**, 150403 (2010).
  - [15] M. Atala, M. Aidelsburger, J. T. Barreiro, D. Abanin, T. Kitagawa, E. Demler, and I. Bloch, *Nat. Phys.* **9**, 795 (2013).
  - [16] M. Cominotti and I. Carusotto, *EPL* **103**, 1001 (2013).
  - [17] N. Fläschner, B. S. Rem, M. Tarnowski, D. Vogel, D.-S. Lühmann, K. Sengstock, and C. Weitenberg, *Science* **352**, 1091 (2016).
  - [18] T. Li, L. Duca, M. Reitter, F. Grusdt, E. Demler, M. Endres, M. Schleier-Smith, I. Bloch, and U. Schneider, *Science* **352**, 1094 (2016).
  - [19] J. Höller and A. Alexandradinata, *Phys. Rev. B* **98**, 24310 (2018).
  - [20] W. Zhang, X. Zhang, Y. V. Kartashov, X. Chen, and F. Ye, *Phys. Rev. A* **97**, 063845 (2018).
  - [21] A. Gómez-León, P. Delplace, and G. Platero, *Phys. Rev. B* **89**, 205408 (2014).
  - [22] N. Goldman and J. Dalibard, *Phys. Rev. X* **4**, 031027 (2014).
  - [23] M. S. Rudner, N. H. Lindner, E. Berg, and M. Levin, *Phys. Rev. X* **3**, 031005 (2013).
  - [24] D. Carpentier, P. Delplace, M. Fruchart, and K. Gawedzki, *Phys. Rev. Lett.* **114**, 106806 (2015).
  - [25] D. J. Thouless, *Phys. Rev. B* **27**, 6083 (1983).
  - [26] T. Kitagawa, E. Berg, M. Rudner, and E. Demler, *Phys. Rev. B* **82**, 235114 (2010).
  - [27] A. M. Dudarev, R. B. Diener, I. Carusotto, and Q. Niu, *Phys. Rev. Lett.* **92**, 153005 (2004).
  - [28] G. Pettini and M. Modugno, *Phys. Rev. A* **83**, 13619 (2011).
  - [29] T. Ozawa and I. Carusotto, *Phys. Rev. Lett.* **112**, 133902 (2014).
  - [30] M. Lohse, C. Schweizer, O. Zilberberg, M. Aidelsburger, and I. Bloch, *Nat. Phys.* **12**, 350 (2016).
  - [31] S. Nakajima, T. Tomita, S. Taie, T. Ichinose, H. Ozawa, L. Wang, M. Troyer, and Y. Takahashi, *Nat. Phys.* **12**, 296 (2016).
  - [32] M. Wimmer, H. M. Price, I. Carusotto, and U. Peschel, *Nat. Phys.* **13**, 545 (2017).
  - [33] M. Aidelsburger, M. Lohse, C. Schweizer, M. Atala, J. T. Barreiro, S. Nascimbène, N. R. Cooper, I. Bloch, and N. Goldman, *Nat. Phys.* **11**, 162 (2014).
  - [34] Y. E. Kraus, Y. Lahini, Z. Ringel, M. Verbin, and O. Zilberberg, *Phys. Rev. Lett.* **109**, 106402 (2012).
  - [35] F. Baboux, E. Levy, A. Lemaître, C. Gómez, E. Galopin, L. Le Gratiet, I. Sagnes, A. Amo, J. Bloch, and E. Akkermans, *Phys. Rev. B* **95**, 161114 (2017).
  - [36] T. Kitagawa, M. A. Broome, A. Fedrizzi, M. S. Rudner, E. Berg, I. Kassal, A. Aspuru-Guzik, E. Demler, and A. G. White, *Nat. Commun.* **3**, 882 (2012).
  - [37] M. Bellec, C. Michel, H. Zhang, S. Tzortzakis, and P. Delplace, *EPL* **119**, 14003 (2017).
  - [38] S. Weidemann, M. Kremer, T. Helbig, T. Hofmann, A. Stegmaier, M. Greiter, R. Thomale, and A. Szameit, *Science* **368**, 311 (2020).
  - [39] See Supplementary material at XXX for a description of the experiment.
  - [40] L. Zhou, C. Chen, and J. Gong, *Phys. Rev. B* **94**, 075443 (2016).
  - [41] J. B. Krieger and G. J. Iafrate, *Phys. Rev. B* **33**, 5494 (1986).